Tungsten nitride thin films prepared by MOCVD

Hsin-Tien Chiu and Shiow-Huey Chuang
Department of Applied Chemistry, National Chiao Tung University, Hsinchu, Taiwan 30050, Republic of China

(Received 16 November 1992; accepted 17 January 1993)

Polycrystalline tungsten nitride thin films were grown by low pressure metallo-organic chemical vapor deposition (MOCVD) using $(^tBuN)_2W(NH^tBu)_2$ as the single-source precursor. Deposition of uniform thin films on glass and silicon substrates was carried out at temperatures 723–923 K in a cold-wall reactor, while the precursor was vaporized at 333–363 K. The growth rates were 2–10 nm/min depending on the condition employed. Bulk elemental composition of the thin films, studied by wavelength dispersive spectroscopy (WDS), is best described as WN_x ($x = 0.7–1.8$). The N/W ratio decreased with increasing temperature of deposition. X-ray diffraction (XRD) studies showed that the films have cubic structures with the lattice parameter $a = 0.414–0.418$ nm. The lattice parameter decreased with decreasing N/W ratio. Stoichiometric WN thin films showed an average lattice parameter a of 0.4154 nm. X-ray photoelectron spectroscopy (XPS) showed that binding energies of the $W_{4f7/2}$, $W_{4f5/2}$, and N_{1s} electrons were 33.0, 35.0, and 397.3 eV, respectively. Elemental distribution within the films, studied by secondary ion mass spectroscopy (SIMS) and Auger spectroscopy depth profilings, was uniform. The SIMS depth profiling also indicated that C and O concentrations were low in the film. Volatile products trapped at 77 K were analyzed by gas chromatography–mass spectroscopy (GC–MS) and nuclear magnetic resonance (NMR). Isobutylene, acetonitrile, hydrogen cyanide, and ammonia were detected in the condensable mixtures. Possible reaction pathways were proposed to speculate the origin of these molecules.

I. INTRODUCTION

Tungsten nitride is a potentially useful material for diffusion barriers and gate electrodes in many modern electronic devices.[1–5] Traditionally, tungsten nitride is prepared using techniques that employ energized particles, i.e., ion implantation, sputtering, ion-beam-assisted deposition, plasma jet spray, and plasma enhanced chemical vapor deposition.[3–7] Alternatively, chemical nitridation of tungsten metal and reduction of WCl_6, WF_6, and WO_3 by NH_3 at high temperatures are employed.[8–11] Unlike many other transition metal nitrides, thin films of tungsten nitride are rarely grown by chemical vapor deposition (CVD).[10,11] We and others showed that organoimido complexes of transition metals can be employed as single-source precursors to grow metal nitride thin films by metallo-organic chemical vapor deposition (MOCVD).[12,13] Here, we report the first example of growing tungsten nitride thin films by low pressure MOCVD employing $(^tBuN)_2W(NH^tBu)_2$, **1**, an organoimido complex of tungsten, as the single-source precursor.[14]

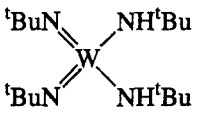

1

II. EXPERIMENTAL

The precursor, $(^tBuN)_2W(NH^tBu)_2$, was prepared according to a published procedure and stored in a dry and oxygen-free environment before further use.[15] A mixture of deuterium-labeled precursors, $(^tBuN)_2W(NH^tBu)_{2-x}(ND^tBu)_x$ ($x = 0–2$), was prepared employing $^tBuNH_{2-x}D_x$ ($x = 0–2$) in the synthesis. The ratio of $(^tBuN)_2W(ND^tBu)_2 : (^tBuN)_2W(ND^tBu)(NH^tBu) : (^tBuN)_2W(NH^tBu)_2$ was 19:44:37, estimated using their mass spectra. Si and glass substrates, cut into squares 1 cm × 1 cm, were cleaned using standard procedures to remove contaminants on the surfaces.

The MOCVD experiments were carried out using a homemade cold-wall reactor. The reactor was heated internally by a 650 W quartz-halogen lamp and evacuated

by a diffusion pumping system. A U-trap was installed between the reactor and the pumping system was used to collect gas phase products at 77 K. For each experiment, a base pressure of 1.33×10^{-3} Pa was obtained before the substrates were loaded under an Ar atmosphere. The reactor was evacuated again while it was heated to a temperature 50 K above the desired temperature of deposition. After the completion of this procedure, the reactor was allowed to cool to the desired temperature of deposition, and the precursor was vaporized into the reactor at 333–363 K. Argon or hydrogen flowing at 10 sccm was used to assist the transport of the precursor into the reactor. Deposition experiments were performed at temperatures 723–923 K for 3 h while the pressures were maintained at ca. 30 Pa. After the flow of **1** was stopped, the films were annealed for 30 min at the same temperature.

The films were analyzed by scanning electron microscopy (SEM), wavelength dispersive spectroscopy (WDS), x-ray diffraction (XRD), Auger electron spectroscopy (AES), x-ray photoelectron spectroscopy (XPS), and secondary ion mass spectroscopy (SIMS). Gas-phase products collected in the experiments were analyzed by gas chromatography–mass spectroscopy (GC–MS) and nuclear magnetic resonance (NMR).

III. RESULTS AND DISCUSSION

A. General deposition and film characteristics

$(^tBuN)_2W(NH^tBu)_2$, a solid compound at room temperature, has sufficient volatility when sublimed between 333 and 363 K under vacuum. The deposition experiments were conducted in a homemade low pressure cold-wall reactor. Ar or H_2 flowing at 10 sccm was used as the carrier gas to assist transportation of the precursor. This resulted in a total pressure (P) of ca. 30 Pa during the experiments. Uniform gray and metallic shining thin films were grown on Si(100), Si(111), and glass substrates between 723 and 923 K. The films on glass substrates showed good adhesion, but some films on silicon substrates did not adhere well (Scotch tape test). This problem was probably due to a large mismatch of lattice parameter between the Si substrates and the thin films. (a_{Si} = 0.543 nm, $a_{thin\ film}$ = 0.414–0.418 nm. See below for $a_{thin\ film}$ determined by XRD.)

Examples of surface and cross-sectional scanning electron micrographs of a typical thin film are shown in Fig. 1. Growth rates, estimated from the cross section of the thin films, were 2–10 nm/min and increased with increasing temperatures of deposition (T_r) and precursor vaporization (T_p). The grain sizes increased with increasing temperature of deposition. At the same temperature of deposition, the growth rate was lower using H_2 than using Ar as the carrier gas.

B. XRD studies

The thin films were polycrystalline as shown by XRD studies. Examples of the XRD patterns of thin films are shown in Fig. 2. Major Cu K_α peaks at angles 2θ equal to 37.14–37.71°, 43.36–43.64°, 63.03–63.42°, and 75.56–76.13° were observed. These peaks are assignable to (111), (200), (220), and (311) reflections of cubic structures with their lattice parameters, a, being 0.4137–0.4175 nm. The data are close to, but higher than, the lattice parameter of β–W_2N, 0.4127 nm.[16] The (111), (200), (220), and (311) reflections of β–W_2N, which has a face-centered cubic sublattice of W atoms with N atoms in the octahedral sites, are at 37.73°, 43.85°, 63.73°, and 76.51°, respectively. The thin films deposited at low temperatures showed broad reflection peaks, probably due to small crystal sizes and distortion of the face-centered cubic lattice structure by extra N atoms (see below for elemental composition). Lattice parameter, a, of the thin films versus the temperature of the deposition is shown in Fig. 3, indicating that a decreased with increasing temperature of deposition.

C. Composition of thin films

Bulk elemental composition of the films was obtained by using WDS. In Fig. 4, N/W and C/W ratios of the thin films, derived from the WDS studies, are plotted against the temperature of deposition. Figure 4 indicates that with increasing temperature of deposition from 773 to 923 K, the N/W ratio decreased from 1.8 to 0.7 while the C/W ratio, which is low, did not change significantly. Dependence of the lattice parameter with the N/W ratio is shown in Fig. 5, which indicates that the lattice parameter decreased with decreasing N/W ratio. The expansion of lattice parameter by increasing the number of N atoms can be rationalized as follows: β–W_2N has a face-centered cubic sublattice of W atoms with half of the octahedral sites occupied by N atoms. For cubic WN observed in this study, the W atoms are in a face-centered cubic sublattice also, but all of the octahedral holes are occupied by the N atoms, causing the lattice parameter to expand to an average of 0.4154 nm. When N/W ratios exceed 1, some N atoms are forced to occupy sites other than the octahedral holes, such as the tetrahedral holes. This distorts and expands the W sublattice further to show broad XRD peaks.

X-ray photoelectron spectra of a thin film are shown in Fig. 6. In Fig. 6(a), a survey of the surface indicates the existence of W, C, N, and O atoms. After several minutes of sputtering by Ar^+, the high resolution spectrum of the W region [Fig. 6(b)] showed major $W_{4f7/2}$ and $W_{4f5/2}$ signals at 32.9 and 35.0 eV, respectively. These values are comparable to those reported for β–W_2N, 33.0 ($W_{4f7/2}$), and 35.0 ($W_{4f5/2}$) eV.[11] The

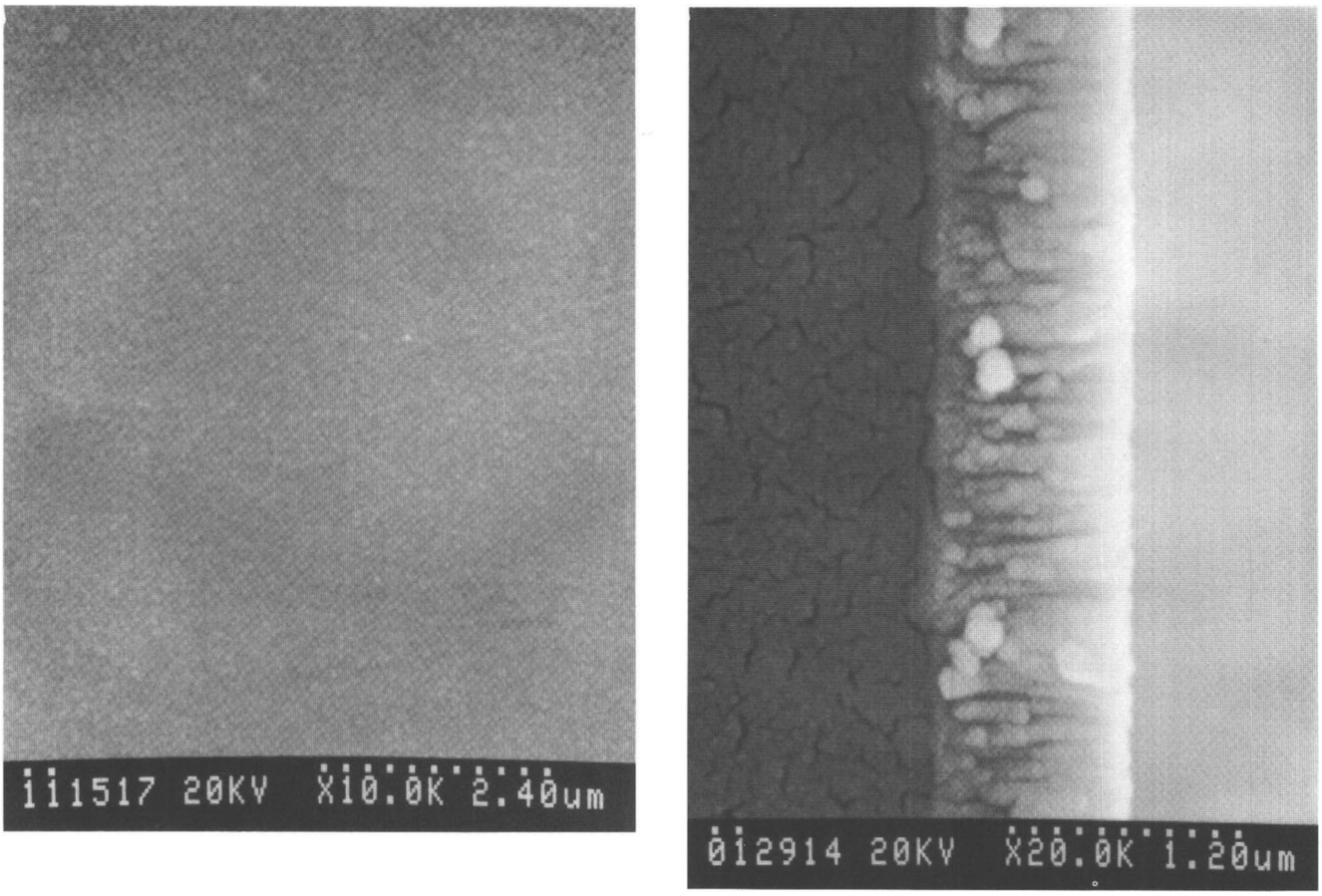

(a) (b)

FIG. 1. (a) Surface SEM photographs of a thin film. Deposited on Si at T_r = 873 K, T_p = 333 K, Ar flow rate = 10 sccm, and P = 30 Pa. (b) Cross-sectional SEM photographs of a thin film. Deposited on Si at T_r = 873 K, T_p = 333 K, H_2 flow rate = 10 sccm, and P = 30 Pa.

surface oxide layers, not removed completely by Ar^+ sputtering, showed a shoulder for $W_{4f5/2}$ electrons at 37.5 eV, while the signal of $W_{4f7/2}$ electrons overlapped with those of the tungsten nitride. The binding energy of O_{1s} electrons was observed at 530.7 eV, close to the value of WO_3, 530.3 eV.[17] The binding energy of N_{1s} electrons [Fig. 6(c)], 397.3 eV, is close to a value reported for $\beta-W_2N$, 397.0 eV.[11] After sputtering by Ar^+, the binding energy of C_{1s} electrons was at 285.8 eV with the peak width at half the peak height equal to 3 eV. This suggests that some C atoms were bound to N and O atoms and some were adventitious carbon atoms from air.

An Auger electron spectrum of a thin film, Fig. 7(a), shows characteristic signals of W, C, N, and O atoms. A depth profile of the sample, Fig. 7(b), indicates that initially, the signals of W and C increased and the signals of N and O decreased with increasing sputtering time. After several minutes of Ar^+ sputtering, all the signals leveled, indicating that the elemental distributions within the film were uniform. However, true elemental distributions are difficult to estimate because preferential removal of N atoms and incorporation of C atoms by Ar^+ sputtering was reported for metal nitrides.[18]

To understand the elemental distributions and the effect of different carrier gases, a SIMS depth profiling was carried out for a specially prepared thin film, as shown in Fig. 8. The film was deposited at 873 K, passing Ar initially for 10 min, then passing H_2 for 10 min. At the surface, high C and O counts, probably due to surface contaminants, were observed. After 400 s of Cs^+ bombardment, uniform secondary ion counts were reached. At 850 s, disturbances in the ion counts were shown, indicating nonuniform elemental distributions at this depth. This probably was caused by changing the carrier gas from Ar to H_2 during the thin-film deposition. Between 850 and 2100 s, the ion counts leveled again until the thin film-substrate interface was reached apparently. Although C and O concentrations could not be estimated quantitatively, their abundances are shown qualitatively in Fig. 8. The C and O concentrations were low in the film, determined by comparing their secondary ion counts (2×10^6 for C, 1×10^6 for O) with those generated at the surface (5×10^8 for C, 7×10^6 for

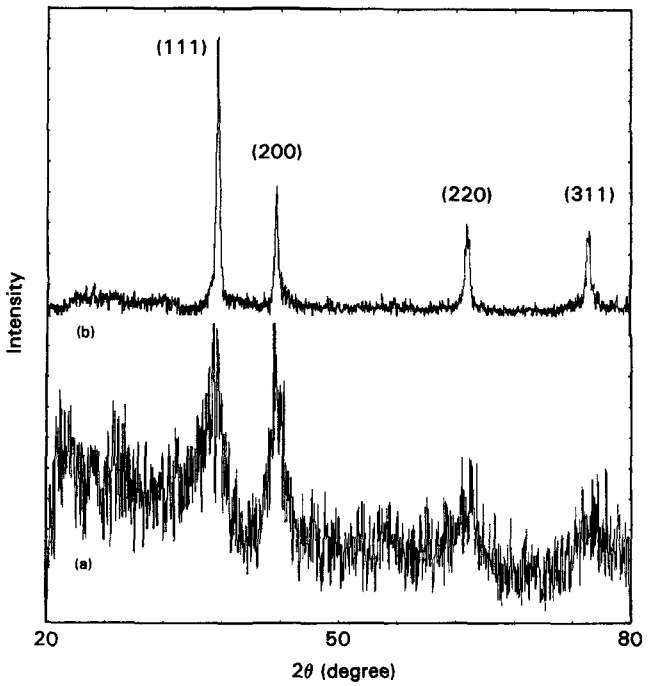

FIG. 2. X-ray diffraction patterns of thin films deposited at (a) 773 K and (b) 873 K on Si at T_p = 333 K, Ar flow rate =10 sccm, and P = 30 Pa.

O) and in the substrate (1×10^6 for both C and O). Employing H_2 as the carrier gas did not affect the elemental distributions within the film, but decreased the growth rate, if the disturbance of the ion counts at 850 s was caused by changing the carrier gas. This is consistent with the growth rates obtained by cross-sectional SEM studies.

Our results shown here are in contrast with a study reported before employing **1** as the precursor to solids.[19]

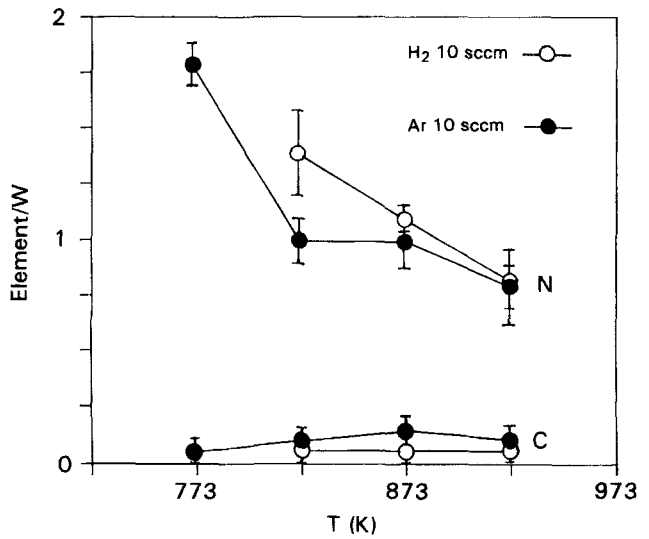

FIG. 3. Effect of temperature of deposition on lattice parameter. T_p = 363 K.

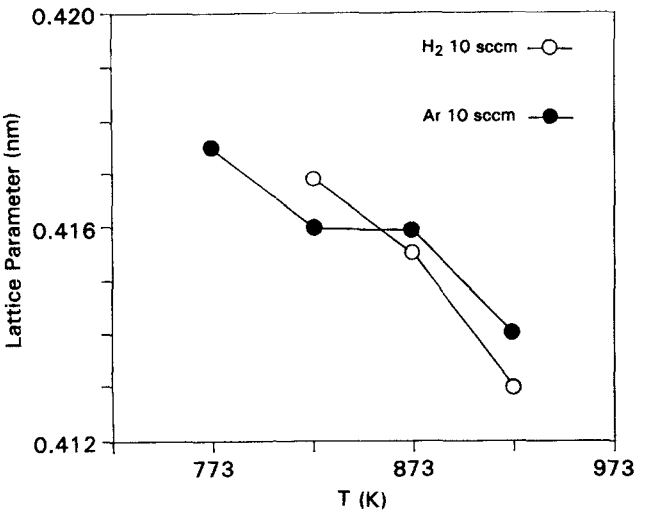

FIG. 4. Effect of temperature of deposition on N/W and C/W ratios. T_p = 363 K.

The solids generated by thermolysis of **1** in NH_3/N_2 atmospheres at 873–1473 K were mixtures of a low percentage of tungsten nitride and a high percentage of tungsten metal (>75 mol %). Decomposition of tungsten nitride into tungsten metal at high temperatures (>1073 K) has been observed.[20] The lower temperatures used in our study ensured that the tungsten nitride thin films did not decompose thermally.

D. Possible reaction pathways

Volatile products condensed at 77 K were analyzed by GC-MS and NMR. The major constituents identified were isobutylene, $Me_2C = CH_2$, and acetonitrile, MeCN, when Ar was used as the carrier gas. In addition to isobutylene and acetonitrile, low concentrations of tertbutylamine, $^tBuNH_2$, ammonia, NH_3, and hydrogen cyanide, HCN, were also detected when H_2 was

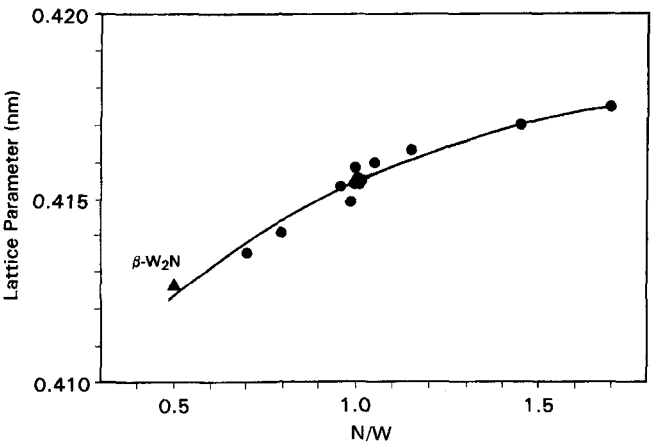

FIG. 5. Dependence of lattice parameter with N/W ratio.

used as the carrier gas. Detection of noncondensable gases, such as hydrogen, nitrogen, and methane, was attempted by installing a pressure gauge between the U-trap and the pump. In the deposition experiments conducted without passing any carrier gas, a pressure increase was observed by this gauge, indicating that the evolution of hydrogen, nitrogen, or methane is possible. When a mixture of deuterium-labeled precursors, $(^tBuN)_2W(ND^tBu)_{2-x}(NH^tBu)_x$ ($x = 0-2$), was employed, evolution of $Me_2C=CH_2$, CH_3CN, and CH_2DCN was observed. NDH_2 was difficult to detect because its molecular weight is the same as water's, which always exists in small quantity in our analytical procedures.

Based on these observations, we speculate that the tertbutylamido and tertbutylimido ligands of **1** dissociated into the volatile hydrocarbons by several different routes, as shown in Eqs. (1)–(3) below.

As suggested in Eqs. (1) and (2), the tertbutyl groups may decompose through γ–hydrogen activation processes. The processes can be called β–hydrogen eliminations if the W–N fragments are part of the surface. Isobutylene is the major organic product here. In Eq. (3), the tertbutyl groups decompose through β–methyl eliminations, probably on the surface, to generate acetonitrile.[21] Further stripping of the methyl group from acetonitrile, followed by combining a surface hydrogen atom, could result in the formation of hydrogen cyanide. Reaction of the $—NH_2$ and $=NH$ groups shown in Eqs. (1) and (2) with H atoms on the surface could account for the generation of NH_3, N_2, and H_2, while the reaction steps involved in Eq. (3) could result in the formation of CH_4. When the deuterium-labeled precursors were employed, $—ND_2$ and $=ND$ groups were formed, according to Eqs. (1) and (2). Then, the D atoms might exchange, probably on the surface, with the H atoms of MeCN to form CH_2DCN.

Addition of excess H_2 into the reaction could hamper the decomposition of $—NH_2$ and $=NH$ into H_2. Alternatively, excess H_2 could generate hydrogen atoms which occupied many active sites on the surface so that the adsorption of **1** was blocked. Both suggestions can rationalize why the growth rates decreased when H_2 was employed as the carrier gas.

The ligands of **1** deserve some comments. Previous attempted syntheses of metal nitrides from transition metal dialkylamido complexes, $M(NR_2)_x$, resulted in the formation of metal carbonitrides instead.[22–24] β–hydrogen activation of the dialkylamido ligands, shown below in Eq. (4), to form metal-carbon bonds was proposed to be responsible for the carbonitride formation.[22] Metal nitrides were obtained only on the occasion of using $M(NR_2)_x$ molecules with NH_3.[25–27] In contrast, each of the ligands of **1** has only one

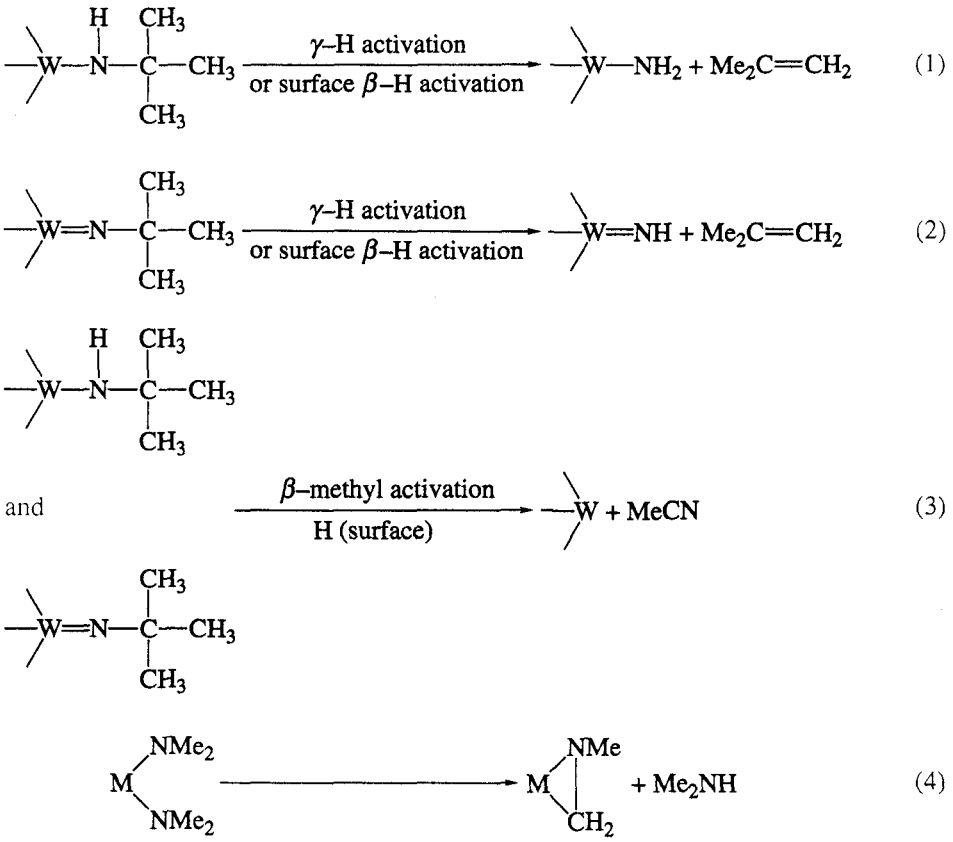

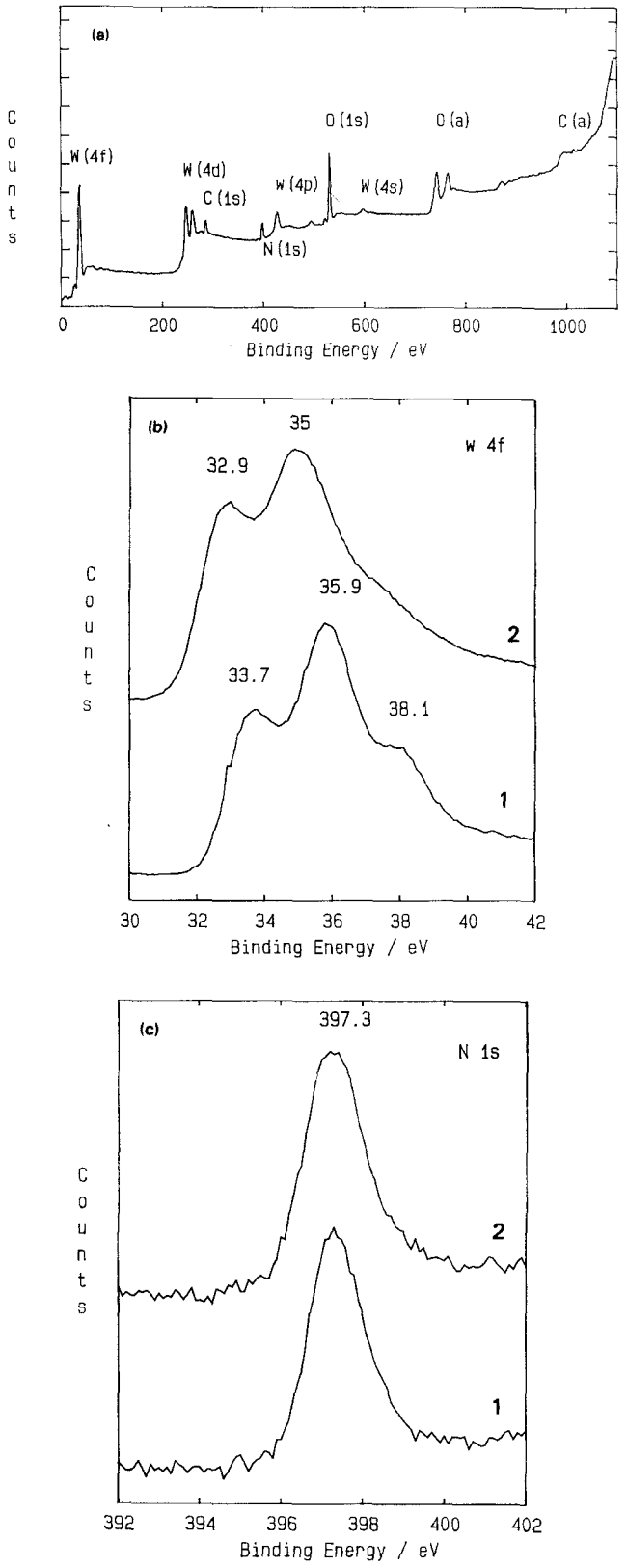

FIG. 6. X-ray photoelectron spectra of a thin film deposited on Si at T_r = 873 K, T_p = 363 K, and H_2 flow rate = 10 sccm. (a) Survey of the sample as-received, (b) W_{4f} region, and (c) N_{1s} region. **1**: as-received and **2**: after sputtering.

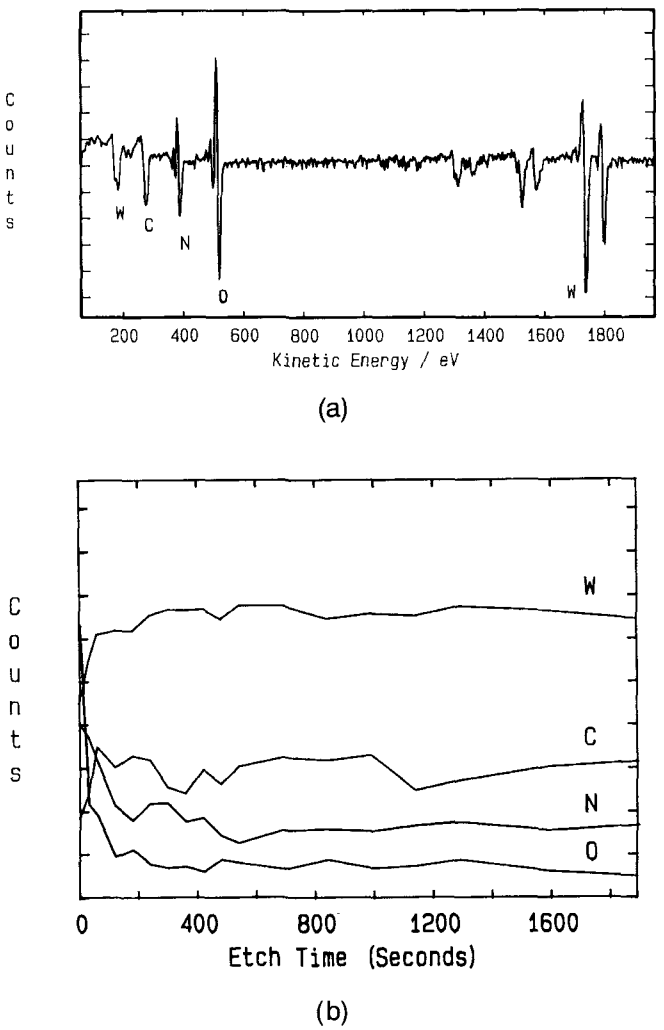

FIG. 7. (a) Auger electron spectrum (as-received) and (b) depth profile of a sample deposited on Si at T_r = 873 K, T_p = 333 K, and H_2 flow rate = 10 sccm.

tertbutyl group connected to the N atom. This reduced the possibility of forming metal-carbon bonds through a pathway analogous to Eq. (4) by the elimination of ^{t}BuNH$_2$. Actually, ^{t}BuNH$_2$ was not a major product in this study. Qualitatively, the doubly bonded tungsten-imido ligand linkage of **1** should be stronger than other M–N single bonds. This would assist to preserve a central "WN" unit through the reaction. A reaction employing Ti(O^{i}Pr)$_4$ to prepare TiO_2 showed little C incorporation.[28] The Ti–O–^{i}Pr linkage of Ti(O^{i}Pr)$_4$ is analogous to the W–N–^{t}Bu linkage of **1**.

How W and N atoms arranged into the cubic lattice is not clear. We speculate that at the initial stage of the reaction, the precursor molecules decomposed thermally to oligomerize into structures analogous to that of $W_4N_4(NPh_2)_6(OC_4H_9)_2$. As shown below, this interesting molecule possesses a W_4N_4 skeleton with two μ_2-N and two μ_3-N atoms bridging the W atoms.[29]

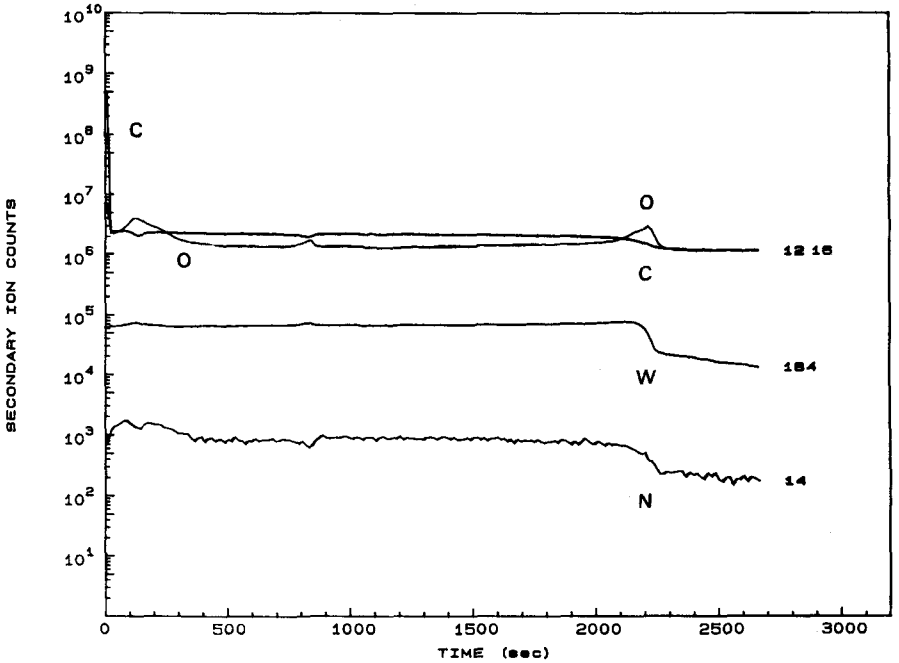

FIG. 8. SIMS depth profile of a thin film deposited on Si at T_r = 873 K, T_p = 363 K, passing Ar (10 sccm) for 10 min, then passing H_2 (10 sccm) for 10 min.

Further expansion of this skeleton three-dimensionally by adding "WN" units will result in a cubic WN lattice.

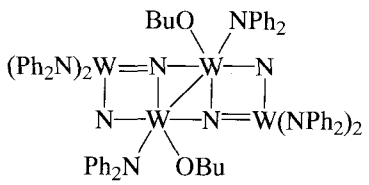

IV. SUMMARY

We have shown that uniform polycrystalline tungsten nitride thin films can be grown successfully from $(^tBuN)_2W(NH^tBu)_2$, a single-source precursor, on glass and silicon substrates by low-pressure MOCVD at 723–923 K. Bulk elemental composition of the thin films, obtained by WDS, is WN_x (x = 0.7–1.8). The N/W ratio decreased with increasing temperature of deposition. XRD studies showed that the films have a cubic structure with the lattice parameter a = 0.414–0.418 nm, slightly larger than that of β–W_2N, 0.4126 nm. Clearly, the lattice parameter decreased with decreasing N/W ratio. A stoichiometric WN thin film has a lattice parameter a equal to 0.4154 nm. XPS studies showed that the binding energies of the $W_{4f7/2}$, $W_{4f5/2}$, and N_{1s} electrons were 33.0, 35.0, and 397.3 eV, respectively, in good agreement with the known values. Elemental distribution within the films is uniform, as shown by SIMS and Auger depth profiling studies. The SIMS depth profiling also indicated that C and O concentrations were low in the film. Volatile products trapped at 77 K were isobutylene, acetonitrile, hydrogen cyanide, and ammonia, as shown by the analyses of GC-MS and NMR. To speculate the origin of these molecules, several C–H, C–C, and C–N activation pathways were proposed.

ACKNOWLEDGMENTS

We thank the National Science Council of the Republic of China (NSC-81-0208-M009-508) for support, and the Instrument Center of the NSC, the Materials Research Laboratory of the ITRI, and the Institute of Materials Science and Engineering of the NCTU for sample analyses.

REFERENCES

1. P. Boher, P. Houdy, P. Kaikati, and L. J. Van Ijzendoorn, J. Vac. Sci. Technol. **A8**, 846 (1990).
2. A. Deneuville, M. Benyahya, M. Brunel, J. C. Oberlin, J. Torres, N. Bourhila, J. Paleau, and B. Canut, Appl. Surf. Sci. **38**, 179 (1989).
3. T. Lalinský, J. Kuzmík, D. Gregušová, Ž. Mozolová, J. Breza, M. Feciško, and P. Seidl, J. Mater. Sci.: Mater. Electron. **3**, 157 (1992).
4. J. S. Lee, C. S. Park, J. W. Yang, J. Y. Kang, and D. S. Ma, J. Appl. Phys. **67**, 1134 (1990).
5. Y. T. Kim and S-K. Min, Appl. Phys. Lett. **53**, 929 (1991).
6. F. M. Kilbane and P. S. Habig, J. Vac. Sci. Technol. **12**, 107 (1975).
7. O. Matsumoto, Y. Shirato, and Y. Hayakawa, J. Electrochem. Soc. Jpn. **37**, 151 (1969).

8. S. Iwama, K. Hayakawa, and T. Arizumi, J. Cryst. Growth **66**, 189 (1984).
9. L. Volpe and M. Boudart, J. Solid State Chem. **59**, 332 (1985).
10. R. L. Landingham and J. H. Austin, J. Less-Comm. Met. **18**, 229 (1969).
11. T. Nakajima, K. Watanabe, and N. Watanabe, J. Electrochem. Soc. **134**, 3175 (1987).
12. H-T. Chiu and W-P. Chang, J. Mater. Sci. Lett. **11**, 96 (1992).
13. C. H. Winter, P. H. Sheridan, T. S. Lewkebandara, M. J. Heeg, and J. W. Proscia, J. Am. Chem. Soc. **114**, 1095 (1992).
14. Preliminary results were communicated; H-T. Chiu and S-H. Chuang, in *Chemical Vapor Deposition of Refractory Metals and Ceramics II,* edited by T. M. Besmann, B. M. Gallois, and J. W. Warren (Mater. Res. Soc. Symp. Proc. **250**, Pittsburgh, PA, 1992), p. 317.
15. W. A. Nugent and R. L. Harlow, Inorg. Chem. **19**, 777 (1980).
16. Powder Diffraction File, JCPDS (International Center for Diffraction Data, Swarthmore, PA, 1982), File No. 25-1257.
17. R. J. Colton and J. W. Rabalais, Inorg. Chem. **15**, 236 (1976).
18. S. Ingrey, M. B. Johnson, R. W. Streater, and G. I. Sproule, J. Vac. Sci. Technol. **20**, 968 (1982)
19. A. L. Currie and K. E. Howard, J. Mater. Sci. **27**, 2739 (1992).
20. M. D. Lyutaya, Poroshk. Metall. (Kiev) **3**, 60 (1979).
21. B. E. Bent, R. G. Nuzzo, and L. H. Dubois, J. Am. Chem. Soc. **111**, 1634 (1989).
22. R. M. Fix, R. G. Gordon, and D. M. Hoffman, Chem. Mater. **2**, 235 (1990).
23. N. M. Rutherford, C. E. Larson, and R. L. Jackson, in *Chemical Perspectives of Microelectronic Materials*, edited by M. E. Gross, J. Jasinski, and J. T. Yates, Jr. (Mater. Res. Soc. Symp. Proc. **131**, Pittsburgh, PA, 1989), p. 439.
24. R. M. Laine and A. S. Hirschon, in *Transformation of Organometallics into Common and Exotic Materials: Design and Activation,* edited by R. M. Laine (Martinus Nijhoff, Dordrecht, The Netherlands, 1988), p. 21.
25. R. M. Fix, R. G. Gordon, and D. M. Hoffman, J. Am. Chem. Soc. **112**, 7833 (1990).
26. R. M. Fix, R. G. Gordon, and D. M. Hoffman, Chem. Mater. **3**, 1138 (1991).
27. R. G. Gordon, U. Riaz, and D. M. Hoffman, J. Mater. Res. **7**, 1679 (1992).
28. J-P. Lu and R. Raj, J. Mater. Res. **6**, 1913 (1991).
29. Z. Gebeyehu, F. Weller, B. Neumüller, and K. Dehnicke, Z. Anorg. Allg. Chem. **593**, 99 (1991).